Molecular Pharmacology Fast Forward. Published on August 13, 2008 as doi:10.1124/mol.108.049056
This article has not been copyedited and formatted. The final version may differ from this version.

Drug binding to the inactivated state is necessary but not sufficient for high affinity binding to hERG channels

Mark J. Perrin, Philip W. Kuchel, Terence J. Campbell, Jamie I. Vandenberg

Mark Cowley Lidwill Research Program in Cardiac Electrophysiology,

Victor Chang Cardiac Research Institute

and

St. Vincent's Clinical School,

University of New South Wales

Mark Cowley Lidwill Research Program in Electrophysiology and Biophysics, Victor Chang Cardiac Research Institute, NSW 2010, Australia (MJP, TJC, JIV)

St Vincent's Clinical School, University of NSW, NSW 2010, Australia (MJP, TJC, JIV)

School of Molecular and Microbial Biosciences, University of Sydney, NSW 2006, Australia (PWK, JIV)

Molecular Pharmacology Fast Forward. Published on August 13, 2008 as DOI: 10.1124/mol.108.049056
This article has not been copyedited and formatted. The final version may differ from this version.

a. **Running title**

State-dependence of drug binding to hERG

b. **Address for correspondence:**

Jamie I Vandenberg
Victor Chang Cardiac Research Institute,
384 Victoria Street,
Darlinghurst, NSW 2010,
Australia
Tel: +61-2-92958371
Fax: +61-2-92958394
Email: j.vandenberg@victorchang.edu.au

c.

number of text pages:	26 (including refs)
number of tables:	2
number of figures:	10
number of references	40
number of words	
Abstract	247
Introduction	609
Discussion	1482

d. **Nonstandard abbreviations used in the paper.**

hERG:	*human ether-a-go-go related gene*
hEAG1:	*human ether-a-go-go gene*
LQTS	long QT syndrome
SQTS	short QT syndrome
WT	wild type
CHO	Chinese Hamster ovary cell
GFP	green fluorescent protein
DMSO	dimethyl sulfoxide
IC_{50}	50% inhibitory concentration

Molecular Pharmacology Fast Forward. Published on August 13, 2008 as DOI: 10.1124/mol.108.049056
This article has not been copyedited and formatted. The final version may differ from this version.

Abstract

Drug block of the human ether à-go-go related gene K^+ channel (hERG) is the most common cause of acquired long QT syndrome, a disorder of cardiac repolarization that may result in ventricular tachycardia and sudden cardiac death. We investigated the open versus inactivated state dependence of drug block by utilizing hERG mutants N588K and N588E, that shift the voltage dependence of inactivation compared to wild-type but where the mutated residue is remote from the drug-binding pocket in the channel pore. Four high affinity drugs (cisapride, dofetilide, terfenadine, astemizole) demonstrated lower affinity for the inactivation-deficient N588K mutant hERG channel compared with N588E and wild type hERG. Three of four low affinity drugs (erythromycin, perhexiline, and quinidine) demonstrated no preference for N588E over N588K channels, while dl-sotalol was an example of a low-affinity state-dependent blocker. All five state-dependent blockers showed an even lower affinity for S620T mutant hERG (no inactivation) compared with N588K mutant hERG (greatly reduced inactivation). Computer modeling indicates that the reduced affinity for S620T compared to N588K and wild type channels can be explained by the relative kinetics of drug block and unblock compared to the kinetics of inactivation and recovery from inactivation. We were also able to calculate, for the first time, the relative affinities for the inactivated versus the open state, which for the drugs tested here ranged from 4-70 fold. Our results show that preferential binding to the inactivated state is necessary but not sufficient for high affinity binding to hERG channels.

Molecular Pharmacology Fast Forward. Published on August 13, 2008 as DOI: 10.1124/mol.108.049056
This article has not been copyedited and formatted. The final version may differ from this version.

The human ether-à-go-go related gene (hERG) encodes the pore-forming subunit of the ion channel that conducts the rapid component of the delayed rectifier potassium current (I_{Kr}) in the heart (Sanguinetti et al., 1995). Gain and loss of function mutations in hERG may result in the clinical conditions of short QT syndrome (SQTS; Brugada et al., 2004) and long QT syndrome (LQTS; Curran et al., 1995) respectively, underscoring the crucial role of hERG in maintaining electrical stability in the heart. The congenital form of LQTS is uncommon and may result from mutations in 10 different genes, most encoding ion channels or their regulatory sub-units (Roden, 2008). Acquired LQTS, through drug-induced blockade of hERG, is more frequent (Sanguinetti et al., 1995; Roden et al., 2004) and a common reason for the withdrawal of medications from the pharmaceutical market (Roden, 2004). Consequently, early assessment of a drug's affinity for hERG has been mandated (Guth, 2007), and obliges the need for a detailed understanding of how drugs bind to hERG.

It is well established that drugs bind in the central cavity of the pore region of hERG (Mitcheson et al., 2000) and that channels need to open before this can occur (Kiehn et al., 1996). At depolarizing potentials, hERG channels can exist in either an open or an inactivated state (Sanguinetti et al., 1995; Smith et al., 1996), yet is has not been established whether the open or the inactivated state is preferred for drug binding. Evidence in support of preferential binding to the inactivated state comes primarily from studies showing reduced affinity for mutant channels that either abolish (S620T; G628C+S631C) or reduce inactivation (S631A) (Ficker et al., 1998; Weerapura et al., 2002). These mutations, however, lie proximate to the selectivity filter and putative drug-binding pocket (see Figure 1) and so may affect drug-block by gating-independent means through local changes in the drug-binding pocket. To address this concern we investigated whether mutations to residues that are remote from the central pore but affect inactivation would also alter drug binding to hERG in a manner similar to that reported for the S631A and S620T mutants. Specifically, we mutated residue N588, located

Molecular Pharmacology Fast Forward. Published on August 13, 2008 as DOI: 10.1124/mol.108.049056
This article has not been copyedited and formatted. The final version may differ from this version.

on the α-helix of the S5P linker (Torres et al., 2003) and thought to be distant from the drug-binding pocket (Yi et al., 2007), to either glutamate (N588E) or lysine (N588K) (Clarke et al., 2006).

In this study we characterized the binding of four high-affinity blockers (dofetilide, cisapride, astemizole, and terfenadine) as well as four low-affinity blockers (quinidine, perhexiline, erythromycin and dl-sotalol). All four high affinity blockers exhibited reduced affinity for the inactivation deficient mutants (N588K and S620T) whereas only dl-sotalol among the low affinity blockers showed reduced affinity for N588K. In all cases where binding was affected by inactivation deficient mutants the affinity for S620T was markedly lower than for N588K mutant channels. A kinetic model of drug binding indicated that the difference between drug binding to wild-type (WT), N588K and S620T channels can be explained by the kinetics of drug block with the affinity for the open state being reduced 4-70 fold compared to the inactivated state depending on the particular drug studied.

Our results show that preferential binding to the inactivated state is necessary but not sufficient for high affinity binding to hERG channels. Further, we propose that the affinity of drugs for the S620T mutant represents their true affinity for the open conformation of the channel and the measured affinity for the WT channel is a weighted average of the affinity for the open and inactivated states. Further, for the first time, we have provided quantitative assessments of the relative affinities of different drugs for the open and inactivated states of hERG.

Molecular Pharmacology Fast Forward. Published on August 13, 2008 as DOI: 10.1124/mol.108.049056
This article has not been copyedited and formatted. The final version may differ from this version.

Materials and Methods

Molecular Biology

Experiments on WT hERG channels were performed using a Chinese hamster ovary (CHO) cell line stably expressing the hERG K^+ channel (hERG cDNA kindly donated by Dr. Gail Robertson) constructed as previously described (Walker et al., 1999a). CHO cells were cultured in D-ME/F12 with 10% FBS and maintained at 37°C in 5% CO_2. Cells were studied at least 24h after being plated on microscope coverslips. Mutant hERG constructs were generated using the Megaprimer PCR method (Clarke et al., 2006). Mutant constructs (N588K, N588E, S631A or S620T) were sequenced to ensure that only the correct mutation had been made and then subcloned into the pIRES2-eGFP vector. Blank CHO cells were plated onto sterilized glass coverslips. After 24h, the cells were transfected with mutant hERG constructs using PolyFect Transfection Reagent (Qiagen) according to the manufacturer's instructions. After transfection, the cells were incubated at 37°C for a minimum of 1 day prior to electrophysiological study. Successfully transfected cells, identified by the expression of eGFP, were studied using the whole-cell configuration of the patch clamp technique.

Electrophysiology

Borosilicate glass tubing patch pipettes, with resistances of 1–4 MΩ when filled with internal solution, were made using a vertical 2-stage puller (PP-830; Narishige, Japan). The internal solution contained (in mM) 120 potassium gluconate, 20 KCl, 1.5 MgATP, 5 EGTA and 10 HEPES (pH 7.3 with KOH). Membrane potentials were adjusted by -15 mV to correct for the junction potential (calculated using the JPcalc algorithm in pClamp 9) between low Cl^- pipette solution and external bath solution (see below). Currents were amplified (Axopatch 200B amplifier; Molecular Devices, Sunnyvale, Ca) and digitized (DigiData 1200; Molecular

Molecular Pharmacology Fast Forward. Published on August 13, 2008 as DOI: 10.1124/mol.108.049056
This article has not been copyedited and formatted. The final version may differ from this version.

Devices) before storage on a personal computer. Capacitance current transients were electronically subtracted, and series resistance compensation was ~80% for all experiments. Current signals were digitized at 5kHz and low-pass filtered at 2 KHz. Some current traces were leak-subtracted off-line. Acquisition was performed using pClamp software.

Solutions and Drugs

Cells were superfused with a Tyrode solution containing (in mM): 130 NaCl, 5 KCl, 1 MgCl, 1 $CaCl_2$, 12.5 Glucose, 10 Hepes. dl-sotalol was purchased from Bristol-Myers Squibb (Victoria, Australia). All other drugs were purchased from Sigma-Aldrich (NSW, Australia). Cisapride, astemizole, terfenadine, erythromycin, dofetilide, and quinidine, were prepared as stock solutions in dimethyl sulfoxide (DMSO) and subsequently diluted as required with superfusate (maximum final DMSO concentration = 0.1% vv^{-1}). dl-sotalol was prepared as a stock solution in Tyrode solution, and perhexiline as a stock solution in methanol. We have previously reported that DMSO at 0.1% vv^{-1} has no effect on the parameters under study (Walker et al., 1999a).

Voltage Protocols

Steady State Inactivation

From a holding potential of -80 mV the membrane voltage was stepped to +40 mV for 3 seconds to fully activate the channels. For cells expressing WT-hERG and N588E-hERG, the second pulse consisted of a voltage step from +40 mV to -160 mV in 10 mV decrements. For cells expressing N588K, a range of +120 mV to -20 mV was employed. For voltage steps to < -30 mV, an exponential curve was fitted to the first phase of deactivation and extrapolated back to the beginning of the second pulse at which point its magnitude represents the current that the channel would have passed if recovery from inactivation were instantaneous. Channel

Molecular Pharmacology Fast Forward. Published on August 13, 2008 as DOI: 10.1124/mol.108.049056
This article has not been copyedited and formatted. The final version may differ from this version.

conductance was plotted against voltage to yield the voltage-dependent steady state inactivation curve (properly, the steady state recovery from inactivation) and the data fitted with a Boltzmann function:

$$\frac{G}{G_{\max}} = \frac{1}{(1+e^{\frac{V_{0.5}-V_t}{k}})} \quad (1)$$

$V_{0.5}$ - half inactivation voltage

k - slope factor

Drug Block

As this was a comparative study, care was taken to ensure similar conditions for drug testing in WT and mutant channels. However, due to the unique gating characteristics of N588E-hERG and N588K-hERG, slight alterations in the voltage protocol and method of measurement were used. Currents were measured with a two-step voltage protocol: a first step to +20 mV for 3 seconds to fully activate the channels and a second step to a negative membrane potential, usually -110 mV (but see below for variations). During this second voltage step hERG channels quickly recover from inactivation and proceed to deactivate. This second step was termed 'revelatory', because it allowed us to estimate the total conductance of activated channels (open and inactivated) after the 3s period of depolarization.

The revelatory step was typically recorded at -110 mV, although in some N588E-hERG cells a voltage step to -120 mV was employed to allow adequate recovery from inactivation for current measurement. Conversely, a less negative voltage was used for a few N588K-hERG cells in order to minimize series resistance errors due to the large activating current in this non-rectifying construct. Drug block was calculated as $I_{[drug]}/I_{control}$, with all currents measured at the end of the activating step. For N588E-hERG and WT-hERG a single

exponential fit was applied to the first part of the current trace during the revelatory step and extrapolated back to the end of the activating step. In this way current was measured at the same time point for all cells.

Voltage-protocols were repeated at 0.1 Hz. Control currents were recorded 3-5 min after patch rupture, i.e. the time take for current levels to stabilize at a steady state level. The first drug was applied, with solution exchange typically taking less than 10s. Recording continued until a new steady state block was reached (typically 2-4 minutes). Between 2 and 4 doses of drug were applied to each cell with most experiments completed within 20 minutes.

Data Analysis

Initial data analysis was performed using the Clampfit module of the pClamp 9.0 software. Subsequent data analysis and preparation of data for figures were performed with Mathematica 6 (Wolfram Technologies). All data are expressed as mean ± S.E.M (n) and statistical significance ($P<0.05$) was determined using paired t-tests.

Molecular Pharmacology Fast Forward. Published on August 13, 2008 as DOI: 10.1124/mol.108.049056
This article has not been copyedited and formatted. The final version may differ from this version.

Results

$V_{0.5}$ of steady state inactivation in WT-hERG, N588E-hERG and N588K hERG expressed in CHO cells.

To investigate the link between drug binding and state dependence we chose to use mutants of residue N588 located in the α-helix of the S5P linker of hERG (Figure 1). This residue has two important features: first, it is though to be located distant to the drug binding pocket (Yi et al., 2007); and second, it is possible to titrate the voltage-dependence of inactivation of the channels by introducing different charges at this residue (Clarke et al., 2006).

Our previous studies of N588 mutant channels were carried out using the *Xenopus laevis* oocyte expression system; however, mammalian cells are the preferred heterologous expression system to use for drug binding studies (Cavalli et al., 2002). Therefore, we first wanted to confirm that the properties of N588 mutant channels were similar in mammalian cells and *Xenopus laevis* oocytes. When expressed in CHO cells, the $V_{0.5}$ of inactivation for N588E-hERG was -114 mV ± 3 mV with a slope factor of -19 mV ± 1 mV (n = 13); the $V_{0.5}$ of inactivation for WT-hERG was -78 mV ± 2 mV with a slope factor of -27 mV ± 2 mV (n = 11); and the $V_{0.5}$ of inactivation for N588K-hERG was 45 mV ± 4 mV with a slope factor of -14 mV ± 1 mV (n = 6) (Figure 2). All values are similar to those reported for Xenopus oocytes (Clarke et al., 2006). The reversal potential for N588K-hERG; -83.4 ± 2.0 mV (n = 5), was slightly shifted compared to that for WT-hERG; -88.5 ± 2.2 mV (n = 10). This is very similar to previous reports (Cordeiro et al., 2005). The N588K-hERG channels are nevertheless still highly selective for K^+ over Na^+. The reversal potential in the N588E-hERG construct could not be determined due to the small magnitude of its activating currents. However, when expressed in oocytes with much larger currents it was found to be similar to

Molecular Pharmacology Fast Forward. Published on August 13, 2008 as DOI: 10.1124/mol.108.049056
This article has not been copyedited and formatted. The final version may differ from this version.

WT-hERG (Clarke et al., 2006). These properties together make N588 mutant constructs ideal for the investigation of inactivation mediated drug-binding to hERG.

High affinity drug binding is modulated by N588 charge mutants

We initially investigated the affinity of four drugs, previously established to block hERG in the low nanomolar range – astemizole (Zhou et al., 1999), cisapride (Mohammad et al., 1997), dofetilide (Kiehn et al., 1996), and terfenadine (Yang et al., 2004) - for N588E-hERG, WT-hERG and N588K-hERG expressed in CHO cells. Figure 3 shows typical examples of WT-, N588E- and N588K-hERG traces under control conditions and after 5 min equilibration with 30 nM cisapride. Percentage of drug-block was measured at the end of the 3s activating step to +20 mV in all cells. This was performed directly in N588K (Figure 3c), or else by fitting a single exponential curve to the first part of the current trace during the revelatory step in N588E-hERG (Figure 3b) and WT-hERG (Figure 3a) and extrapolating this back to the end of the activating step. The data in Figure 3 indicate that 30 nM cisapride caused less block of N588K-hERG channels compared to N588E- or WT-hERG. This is more clearly seen from the summary Hill-plots shown in Figure 4; cisapride affinity for WT-hERG: 20.5 ± 2.2 nM (n = 4) was similar to that for N588E-hERG: 13.1± 4.9 nM (n = 4) but significantly reduced for N588K-hERG: 55.9 ± 4.2 nM (n = 4). All four high-affinity blockers showed a similar pattern of reduced affinity for N588K- compared to WT- and N588E-hERG (see Figure 4). The affinities for all drugs for WT and N588 mutant constructs are summarized in Table 1.

Low affinity drug binding to N588 charge mutants

We next investigated the affinity of 4 drugs previously established to block hERG in the high nanomolar or micromolar range – quinidine (Lees-Miller et al., 2000), perhexiline (Walker et

Molecular Pharmacology Fast Forward. Published on August 13, 2008 as DOI: 10.1124/mol.108.049056
This article has not been copyedited and formatted. The final version may differ from this version.

al., 1999b), erythromycin (Volberg et al., 2002), and dl-sotalol (Kirsch et al., 2004) - for N588E-hERG, WT-hERG and N588K-hERG constructs expressed in CHO cells. Typical examples of current traces recorded from WT-, N588K- and N588E-hERG in the presence and absence of 3 μM quinidine are illustrated in Figure 5. Quinidine caused a similar degree of block of WT and the two N588 charge mutants. This is also seen from the summary Hill plots (Figure 6A). Perhexiline and erythromycin showed the same pattern as that observed for quinidine, i.e. similar affinities for all hERG constructs (Figure 6A, C). In contrast, dl-sotalol showed a significantly higher affinity for N588E-hERG and WT-hERG compared to N588K-hERG (Figure 6D, Table 1).

Does reduced affinity for N588K-hERG reflect state-dependent binding?

The data from Figures 3 and 4 clearly demonstrate that the four high-affinity drugs used in this study had reduced affinity for the inactivation-deficient N588K-hERG channels. To determine whether this reduced affinity for N588K-hERG reflected a state-dependence of drug-binding we investigated whether there was a similarly reduced affinity for a range of inactivation-deficient mutants. Specifically, we investigated binding of dofetilide to S631A-hERG and S620T-hERG. S631A-hERG has a markedly right-shifted $V_{0.5}$ of steady state inactivation compared to WT-hERG that is very similar to that observed for N588K (Figure 7A) whereas S620T-hERG does not inactivate at measurable voltages (Ficker et al., 1998). Accordingly, at +20 mV, the proportion of channels in the open:inactivated states is ~85:15 for N588K and S631A, compared to 100:0 for S620T, but 2:98 for WT-hERG (Figure 7A).

The affinity of dofetilide for S631A-hERG was not statistically different to that for N588K-hERG (404 ± 95 nM (n = 4), and 377 ± 69 nM (n = 4) respectively), an 8-fold reduction compared to WT-hERG. That these two mutants, with very similar effects on inactivation but apparently not located near each other, have very similar effects on drug

Molecular Pharmacology Fast Forward. Published on August 13, 2008 as DOI: 10.1124/mol.108.049056
This article has not been copyedited and formatted. The final version may differ from this version.

binding suggests that the reduced affinity for drug binding is mediated by reduced inactivation of the channel. However, the affinity of dofetilide for S620T, was reduced a further 10 fold (3494 nM ± 374 nM, n = 4) (Figure 7B) compared to its affinity for S631A or N588K. Given that there is relatively little difference in the extent to which S631A and N588K channels occupy the open state at +20 mV (the voltage at which we assayed drug binding) compared to S620T channels (i.e. ~85% compared to 100%), a marked reduction in drug-affinity for S620T-hERG suggests a gating-independent effect on drug binding by this mutant. An alternative hypothesis is that, despite the relative infrequency with which S631A and N588K channels occupy the inactivated state at +20 mV, the kinetics of drug binding and unbinding are such that whenever the channel enters the inactivated state it binds drug that, with a very slow off rate, remains bound for a long period. According to this hypothesis, binding of drug to the S620T mutant would only encounter the open state and so reflect the affinity for the open state, whereas binding to WT or N588K channels would reflect a weighted average of the affinity for the inactivated and open states dependent on the relative rates of transitions between the two states and drug binding and unbinding rates. To test this hypothesis we set up a computer model of drug binding to hERG channels as depicted in Figure 8.

Modeling kinetics of drug binding to open and inactivated states

The Markov chain model for hERG kinetics is based on that developed by Lu et al. (2001) with the addition of two states: drug-bound open state and drug-bound inactivated state (Figure 8). The rate constants, scaled to 22°C, for the model are tabulated in the data supplement. To model the S620T mutant the rate constants for transition steps to the inactivated state were set to 0. To model the N588K mutant, the rate constants for the transition between the open and inactivated states were adjusted to reproduce the

Molecular Pharmacology Fast Forward. Published on August 13, 2008 as DOI: 10.1124/mol.108.049056
This article has not been copyedited and formatted. The final version may differ from this version.

experimentally observed changes in these rate constants and the steady-state inactivation (see data supplement). For simplicity, we assumed that the kinetics of activation were the same for WT-, S620T- and N588K-hERG channels.

To calculate the rate constants for open and inactivated drug blocked state we assumed that drug affinity for S620T represented the affinity for the open state. The rate constants for open state drug block, *kf6* and *kb6*, were constrained to fit the data for drug binding to the S620T channels. The values for *kf6* and *kb6* were then held constant and the values for drug binding to the inactivated state, *kf7* and *kb7*, constrained to fit the time course of drug block for WT channels. In the case of dofetilide binding, the calculated affinity for the open state (*kf6*/*kb6*) was 3.5 μM, i.e. the value for S620T, and the calculated affinity for the inactivated state (*kf7*/*kb7*) was 47.8 nM. The measured affinity for dofetilide binding to WT channels, 50.1 nM, is much closer to the calculated value for the affinity to the inactivated state reflecting both the greater proportion of time WT channels spend in the inactivated state and the slower dissociation of drug from the inactivated state. If the original assumption was correct, i.e. drug affinity for S620T is the true affinity of the drug for the open state, then substitution of the values for *kf6*, *kb6*, *kf7* and *kb7* into our model for N588K should reproduce the experimentally determined IC_{50} for dofetilide binding to N588K. As can be seen from the data in Figure 9, the model predicted values are very close to the experimental data. The same procedure was repeated for each of the state-dependent drugs formerly assessed (Figure 10A-D) with similarly good approximations to the experimental data.

Molecular Pharmacology Fast Forward. Published on August 13, 2008 as DOI: 10.1124/mol.108.049056
This article has not been copyedited and formatted. The final version may differ from this version.

Discussion

State-dependence of drug binding

Most drugs that block hERG require channel opening (Kiehn et al., 1996). Some evidence suggests that, once activated, inactivation increases drug affinity for the channel: first, mutant hERG channels with disrupted inactivation (S631A, S620T, and G628C/S631C) reduce drug-block by multiple agents (Ficker et al., 1998; Lees-Miller et al., 2000; Numaguchi et al., 2000; Yang et al., 2004); second, mutations introduced into Bovine-EAG (bEAG) and hEAG1 that enable inactivation also confer sensitivity to dofetilide block (Ficker et al., 2001, Gómez-Varela et al., 2006). However, the inactivation disrupting mutations could affect drug-block through gating-independent means. S631 and S620 lie proximate to the drug-binding space, and mutations at these positions may produce conformational changes at the base of the pore helix – an important molecular determinant of drug-binding (Mitcheson et al., 2000). G628C/S631C markedly reduces the potassium selectivity of hERG (Smith et al., 1996), suggesting a conformational change in the vicinity of the selectivity filter. Further, mutant hERG channels G648A and T623A promote inactivation, but reduce methanesulfonamide block of hERG (Mitcheson et al., 2000). In addition, voltage protocols designed to favor occupancy of the inactivated state during drug-binding (i.e. large depolarizations) also relieve drug block (Kiehn et al., 1996; Numaguchi et al., 2000).

The data reported in this study provides strong evidence that drug-binding to hERG K^+ channels is influenced by whether the channels are in the inactivated or the open state. In addition, we have demonstrated that this phenomenon is drug-dependent, with the ratio of affinities for the open to inactivated state varying from 1:1 (i.e. not state-dependent: quinidine, erythromycin, perhexiline) to 1:70 (dofetilide).” First, we have shown that a mutation, N588K, introduced into a region thought to be remote from the drug-binding pocket

Molecular Pharmacology Fast Forward. Published on August 13, 2008 as DOI: 10.1124/mol.108.049056
This article has not been copyedited and formatted. The final version may differ from this version.

(Yi et al., 2007) that shifts the voltage-dependence of inactivation (Brugada et al., 2004; Clarke et al., 2006) affects drug-binding. A combination of structural studies (Torres et al., 2003), toxin binding studies (Pardo-Lopez et al., 2002) and molecular dynamics modeling studies (Yi et al., 2007) suggest that N588 on the hydrophilic surface of the S5P α-helix faces the extracellular space and is therefore remote from the drug-binding pocket. Second, we have shown that two distinct mutants that have very similar effects on inactivation (N588K and S631A) have similar effects on drug-binding. The simplest explanation is that it is the effect these mutations have on inactivation that accounts for the altered drug-binding. Third, our kinetic modeling of drug-binding to WT, S620T and N588K mutant channels demonstrates that all the differences in drug-binding between these mutants can be explained on the basis of differences in occupancy of open and inactivated states and the kinetics of drug-binding. Our kinetic modeling studies have also enabled, for the first time, estimation of the binding affinities for both the open and inactivated states for a range of drugs.

Stork et al. (2008) have recently published data extending the concept of state dependence to the dissociation of drugs from the hERG channel. As they have elegantly shown, some drugs require opening of the activation gate to dissociate from the inner cavity of the channel. Our data is complementary to their own, demonstrating that the rate of drug dissociation will depend not only on the relative proportions of activated and closed channels at a given voltage, but also the proportion of activated channels in the inactivated or open state, itself a function of voltage.

In contrast with our data, there is one report in the literature that suggests mutations to S620 could have a gating-independent effect on drug-binding (Guo et al., 2006). Guo and colleagues showed that S620T and S620C both abolished inactivation gating but had different affinities for E-4031 – a methanesulfonamide similar to dofetilide. This data, however, is not necessarily incompatible with our results. It is possible that the abolition of inactivation alters

Molecular Pharmacology Fast Forward. Published on August 13, 2008 as DOI: 10.1124/mol.108.049056
This article has not been copyedited and formatted. The final version may differ from this version.

drug affinity in both the S620T and S620C. However, whereas the S620T represents the true affinity for the open state, the cysteine side chain in S620C, is able to bind to the drug and thereby increase the affinity relative to that for S620T.

What explains the strong preference for inactivated state binding?

The molecular determinants of drug-binding to hERG include two aromatic residues in the S6 helix, F656 and Y652; and to a variable extent: three residues close to the selectivity filter: T623, S624, V625, and two residues in S6: G648, and V659 (Figure 1). In the absence of a high-resolution structure of hERG, the exact conformation of these residues in relation to each other cannot be determined. It has been suggested that inactivation of hERG channels involves changes in the structure of the pore region (Chen et al., 2002), and so the spatial relationships of the different components of the drug-binding pocket are likely to vary between the open and inactivated state. One can imagine two scenarios that could arise. First, a conformational change around the selectivity filter and base of the pore-helix secondary to inactivation (as has been suggested to occur in hERG; Gang & Zhang, 2006) could result in a reorientation of the drug-binding residues at the base of the selectivity filter relative to the drug-binding residues on S6.

Second, inactivation could involve reorientation of the S6 helixes, relative to their positions in the open state. In this hypothesis not only would the relationship between the drug-binding residues on S6, Y652 and F656, alter with respect to drug-binding residues at the base of the pore-helixes (Chen et al., 2002; Lees-Miller et al., 2000), but also the inter-subunit relationships between Y652 and F656 would change (Myokai et al., 2008). Evidence in favor of a primary role for reorientation of S6 in favoring inactivated state drug-binding comes from a study investigating the effect of mutating F656 to methionine on the binding of droperidol (Luo et al., 2008). The affinity of droperidol for S631A-hERG was reduced

Molecular Pharmacology Fast Forward. Published on August 13, 2008 as DOI: 10.1124/mol.108.049056
This article has not been copyedited and formatted. The final version may differ from this version.

compared to WT-hERG, but introduction of S631A into the background of the F656M mutant did not reduce the affinity compared to F656M-hERG alone.

The reduction in affinity of dofetilide for S620T-hERG compared to WT-hERG (70-fold) is comparable to the reduction in drug-affinities seen when residues Y652 or F656 are mutated (Mitcheson et al., 2000; Lees-Miller et al., 2000). This suggests that abolition of inactivation results in the complete elimination of one of the interactions between dofetilide and the channel. However, for astemizole, cisapride, sotalol and terfenadine the reduction in affinity is more modest suggesting an interaction has been reduced but not eliminated.

Inactivated state binding is necessary but not sufficient for high affinity binding

All the high affinity blockers tested in this study showed a marked preference for the inactivated state. At depolarized potentials, WT-hERG channels predominantly reside in the inactivated state therefore it is unsurprising that the drugs with the highest affinity for the inactivated state show the highest affinity for WT-hERG. However, our data for dl-sotalol clearly indicates that state-dependence of binding is not sufficient to produce high affinity binding. One plausible explanation for the low affinity yet state-dependence of dl-sotalol binding is that it binds to the residues most critical for state-dependent binding but does not bind to any other residues whereas the higher affinity state-dependent blockers bind both to the critical state-dependent residues as well as others. If this hypothesis is correct, then determining the molecular basis of sotalol binding to hERG would be a useful probe for determining the minimum requirements for state-dependent binding to hERG.

Relevance for drug-binding in SQTS

The most common form of short QT syndrome (SQTS) results from the N588K mutation in hERG (Brugada et al., 2004). The wide spectrum of drugs known to block hERG provides

multiple candidates for treatment. However, initial testing demonstrated that d-sotalol failed to prolong the QT interval (Brugada et al., 2004). Of tested candidates, only quinidine (Gaita et al., 2004), disopyramide (McPate et al., 2006), and doxepin (Duncan et al., 2007) have been shown to block N588K at affinities similar to WT. Of significance, all block hERG in the micromolar (low affinity) range. Of note, although the binding affinity of astemizole for N588K is reduced compared to WT, its affinity for N588K is 250 fold greater than quinidine. Combined with a benign side-effect profile, it is a good candidate for evaluation as a treatment for SQTS type 1.

Relevance for high throughput assays

Given the mandated need to screen all drugs for hERG binding, there has been considerable effort put into developing high throughput screens for assaying drug-binding to hERG (Dorn et al., 2005; Tang et al., 2001). In general, however, the results of these screens have been poor and we suggest that this may be because they predominantly assay binding to the open state and therefore underestimate the affinity of drugs that preferentially bind the inactivated state. Given that the difference in affinity between the open and inactivated states can be 70-fold, it is important that any high throughput screening system must assay binding to the inactivated state.

Molecular Pharmacology Fast Forward. Published on August 13, 2008 as DOI: 10.1124/mol.108.049056
This article has not been copyedited and formatted. The final version may differ from this version.

Conclusions

We investigated the relationship between inactivation gating and drug-block of hERG, finding that high affinity block (nanomolar range) is promoted by inactivation. The use of charged mutants at N588 provides a methodology for investigating the conformational changes of the channel pore between open and inactivated states. Further, we have calculated for the first time the relative affinities of drug-binding to the open and inactivated states of the hERG channel, which in the case of dofetilide shows a 70-fold greater affinity for the inactivated state. The pharmaceutical importance of these data is highlighted by the observation that two drugs (astemizole and terfenadine) that have been withdrawn from the market, and one (cisapride) that has had its use severely restricted, exhibit a marked preference for binding to the inactivated state. In this study we have also identified astemizole as a high affinity blocker of the mutant N588K-hERG channel, and propose it as a possible therapeutic candidate for treatment of the life threatening SQTS 1.

Molecular Pharmacology Fast Forward. Published on August 13, 2008 as DOI: 10.1124/mol.108.049056
This article has not been copyedited and formatted. The final version may differ from this version.

Acknowledgements

We would like to thank Jane Bursill, Adam Hill, Stefan Mann, Tadeusz Marciniec and Ken Wyse for excellent technical assistance and Catherine Clarke, Mark Hunter and JingTing Zhao for useful discussions.

Molecular Pharmacology Fast Forward. Published on August 13, 2008 as DOI: 10.1124/mol.108.049056
This article has not been copyedited and formatted. The final version may differ from this version.

References

Brugada R, Hong K, Dumaine R, Cordeiro J, Gaita F, Borggrefe M, Menendez TM, Brugada J, Pollevick GD, Wolpert C, Burashnikov E, Matsuo K, Wu YS, Guerchicoff A, Bianchi F, Giustetto C, Schimpf R, Brugada P and Antzelevitch C (2004) Sudden death associated with short-QT syndrome linked to mutations in HERG. *Circulation* **109(1)**:30–35.

Cavalli A, Poluzzi E, De Ponti F and Recanatini M (2002) Toward a pharmacophore for drugs inducing the long QT syndrome: insights from a CoMFA study of HERG K(+) channel blockers. *J Med Chem* **45(18)**:3844–3853.

Chen J, Seebohm G and Sanguinetti MC (2002) Position of aromatic residues in the S6 domain, not inactivation, dictates cisapride sensitivity of HERG and eag potassium channels. *Proc Natl Acad Sci U S A* **99(19)**:12461–12466.

Clarke CE, Hill AP, Zhao J, Kondo M, Subbiah RN, Campbell TJ and Vandenberg JI (2006) Effect of S5P alpha-helix charge mutants on inactivation of hERG K+ channels. *J Physiol* **573(Pt 2)**:291–304.

Cordeiro JM, Brugada R, Wu YS, Hong K and Dumaine R (2005) Modulation of I(Kr) inactivation by mutation N588K in KCNH2: a link to arrhythmogenesis in short QT syndrome. *Cardiovasc Res* **67(3)**:498–509.

Curran ME, Splawski I, Timothy KW, Vincent GM, Green ED and Keating MT (1995) A molecular basis for cardiac arrhythmia: HERG mutations cause long QT syndrome. *Cell* **80(5)**:795–803.

Dorn A, Hermann F, Ebneth A, Bothmann H, Trube G, Christensen K and Apfel C (2005) Evaluation of a high-throughput fluorescence assay method for HERG potassium channel inhibition. *J Biomol Screen* **10(4)**:339–347.

Duncan RS, McPate MJ, Ridley JM, Gao Z, James AF, Leishman DJ, Leaney JL, Witchel HJ and Hancox JC (2007) Inhibition of the HERG potassium channel by the tricyclic antidepressant doxepin. *Biochem Pharmacol* **74(3)**:425–437.

Ficker E, Jarolimek W and Brown A (2001) Molecular determinants of inactivation and dofetilide block in ether a-go-go (EAG) channels and EAG-related K(+) channels. *Mol Pharmacol* **60(6)**:1343–1348.

Ficker E, Jarolimek W, Kiehn J, Baumann A and Brown AM (1998) Molecular determinants of dofetilide block of HERG K+ channels. *Circ Res* **82(3)**:386–395.

Gaita F, Giustetto C, Bianchi F, Schimpf R, Haissaguerre M, Calo L, Brugada R, Antzelevitch C, Borggrefe M and Wolpert C (2004) Short QT syndrome: pharmacological treatment. *J Am Coll Cardiol* **43(8)**:1494–1499.

Gomez-Varela D, Contreras-Jurado C, Furini S, Garcia-Ferreiro R, Stuhmer W, and Pardo LA (2006) Different relevance of inactivation and F468 residue in the mechanisms of hEag1

channel blockage by astemizole, imipramine and dofetilide. *FEBS Lett* **580(21)**:5059–5066.

Guo J, Gang H and Zhang S (2006) Molecular determinants of cocaine block of human ether-a-go-go-related gene potassium channels. *J Pharmacol Exp Ther* **317(2)**:865–874.

Guth BD (2007) Preclinical cardiovascular risk assessment in modern drug development. *Toxicol Sci* **97(1)**:4–20.

Kiehn J, Lacerda AE, Wible B and Brown AM (1996) Molecular physiology and pharmacology of HERG. Single-channel currents and block by dofetilide. *Circulation* **94(10)**:2572–2579.

Kirsch GE, Trepakova ES, Brimecombe JC, Sidach SS, Erickson HD, Kochan MC, Shyjka LM, Lacerda AE and Brown AM (2004) Variability in the measurement of hERG potassium channel inhibition: effects of temperature and stimulus pattern. *J Pharmacol Toxicol Methods* **50(2)**:93–101.

Lees-Miller J, Duan Y, Teng G, and Duff H (2000) Molecular determinant of high-affinity dofetilide binding to HERG1 expressed in Xenopus oocytes: involvement of S6 sites. *Mol Pharmacol* **57(2)**:367-374.

Lu Y, Mahaut-Smith MP, Varghese A, Huang CL, Kemp PR and Vandenberg JI (2001) Effects of premature stimulation on HERG K(+) channels. *J Physiol* **537(Pt 3)**:843–851.

Luo T, Luo A, Liu M and Liu X (2008) Inhibition of the HERG channel by droperidol depends on channel gating and involves the S6 residue F656. *Anesth Analg* **106(4)**:1161–1170.

McPate M, Duncan R, Witchel H and Hancox J (2006) Disopyramide is an effective inhibitor of mutant HERG K+ channels involved in variant 1 short QT syndrome. *J Mol Cell Cardiol* **41(3)**:563–566.

Mitcheson JS, Chen J, Lin M, Culberson C and Sanguinetti MC (2000) A structural basis for drug-induced long QT syndrome. *Proc Natl Acad Sci U S A* **97(22)**:12329–12333.

Mitcheson J (2008) hERG Potassium Channels and the Structural Basis of Drug-Induced Arrhythmias. *Chem Res Toxicol In Press* (DOI: 10.1021/tx800035b)

Mohammad S, Zhou Z, Gong Q and January CT (1997) Blockage of the HERG human cardiac K+ channel by the gastrointestinal prokinetic agent cisapride. *Am J Physiol* **273(5 Pt 2)**:H2534–8.

Myokai T, Ryu S, Shimizu H and Oiki S (2008) Topological mapping of the asymmetric drug-binding to the HERG potassium channel by use of tandem dimers. *Mol Pharmacol* . (DOI: 10.1124/mol.107.042085)

Numaguchi H, Mullins F, Johnson JJ, Johns D, Po S, Yang I, Tomaselli G, and Balser J (2000) Probing the interaction between inactivation gating and Dd-sotalol block of HERG. *Circ Res* **87(11)**:1012-1018.

Pardo-Lopez L, Zhang M, Liu J, Jiang M, Possani LD and Tseng GN (2002) Mapping the binding site of a human ether-a-go-go-related gene-specific peptide toxin (ErgTx) to the channel's outer vestibule. *J Biol Chem* **277(19)**:16403–16411.

Roden DM (2004) Drug-induced prolongation of the QT interval. *N Engl J Med* **350(10)**:1013–1022.

Roden DM (2008) Clinical practice. Long-QT syndrome. *N Engl J Med* **358(2)**:169–176.

Sanguinetti M, Jiang C, Curran M and Keating M (1995) A mechanistic link between an inherited and an acquired cardiac arrhythmia: HERG encodes the IKr potassium channel. *Cell* **81(2)**:299–307.

Smith P, Baukrowitz T and Yellen G (1996) The inward rectification mechanism of the HERG cardiac potassium channel. *Nature* **379(6568)**:833–836.

Stork D, Timin EN, Berjukow S, Huber C, Hohaus A, Auer M, and Hering S (2007) State dependent dissociation of HERG channel inhibitors. *Br J Pharmacol* **151(8)**:1368–1376.

Tang W, Kang J, Wu X, Rampe D, Wang L, Shen H, Li Z, Dunnington D and Garyantes T (2001) Development and evaluation of high throughput functional assay methods for HERG potassium channel. *J Biomol Screen* **6(5)**:325–331.

Torres AM, Bansal PS, Sunde M, Clarke CE, Bursill JA, Smith DJ, Bauskin A, Breit SN,

Campbell TJ, Alewood PF, Kuchel PW and Vandenberg JI (2003) Structure of the HERG K+ channel S5P extracellular linker: role of an amphipathic alpha-helix in C-type inactivation. *J Biol Chem* **278(43)**:42136–42148.

Volberg WA, Koci BJ, Su W, Lin J and Zhou J (2002) Blockade of human cardiac potassium channel human ether-a-go-go-related gene (HERG) by macrolide antibiotics. *J Pharmacol Exp Ther* **302(1)**:320–327.

Walker B, Singleton C, Bursill J, Wyse K, Valenzuela S, Qiu M, Breit S and Campbell T (1999a) Inhibition of the human ether-a-go-go-related gene (HERG) potassium channel by cisapride: affinity for open and inactivated states. *Br J Pharmacol* **128(2)**:444–450.

Walker B, Valenzuela S, Singleton C, Tie H, Bursill J, Wyse K, Qiu M, Breit S and Campbell T (1999b) Inhibition of HERG channels stably expressed in a mammalian cell line by the antianginal agent perhexiline maleate. *Br J Pharmacol* **127(1)**:243–251.

Weerapura M, Hebert T and Nattel S (2002) Dofetilide block involves interactions with open and inactivated states of HERG channels. *Pflugers Arch* **443(4)**:520–531.

Yang B, Xu D, Xu C, Li Z, Du Z, Wang H and Dong D (2004) Inactivation gating determines drug potency: a common mechanism for drug blockade of HERG channels. *Acta Pharmacol Sin* **25(5)**:554–560.

Yi H, Cao Z, Yin S, Dai C, Wu Y and Li W (2007) Interaction simulation of hERG K+ channel with its specific BeKm-1 peptide: insights into the selectivity of molecular

recognition. *J Proteome Res* **6(2)**:611–620.

Zhou Z, Vorperian VR, Gong Q, Zhang S and January CT (1999) Block of HERG potassium channels by the antihistamine astemizole and its metabolites desmethylastemizole and norastemizole. *J Cardiovasc Electrophysiol* **10(6)**:836–843.

Footnotes

* This work was supported in part by project grants from the St Vincent's Clinic Foundation (to TJC) and a Widdifield Cardiac Research Scholarship to MJP. JIV is a National Health and Medical Research Council Senior Research Fellow.

Address for reprint requests

Jamie I Vandenberg

Victor Chang Cardiac Research Institute,

384 Victoria Street,

Darlinghurst, NSW 2010,

Australia

Email: j.vandenberg@victorchang.edu.au

Molecular Pharmacology Fast Forward. Published on August 13, 2008 as DOI: 10.1124/mol.108.049056
This article has not been copyedited and formatted. The final version may differ from this version.

Figure Legends

Figure 1: Schematic diagram of the S5, S6, pore helix, and S5P linker regions of two hERG subunits. The most important molecular determinants of drug-block are denoted with grey circles. Commonly employed mutants that disrupt inactivation are displayed with white stars. Note that G648 is probably not exposed to the pore cavity, and is thought to influence drug block by determining the conformation of the drug-binding pocket; V659 may influence drug-block by altering the gating characteristics of the channel (Mitcheson 2000; Mitcheson, 2008). The S5P linker is dashed, as its exact position relative to the pore is unknown.

Figure 2: Conductance voltage curves for N588E-hERG (○), WT-hERG (■), and N588K-hERG (●). Data points are mean ± S.E.M and the curve fitted to the data is a Boltzmann function with a $V_{0.5}$ of inactivation of -114 ± 3 mV and slope factor of -19 mV (n = 13) for N588E-hERG, $V_{0.5}$ of -78 ± 2 mV and slope factor of -26 mV (n = 11) for WT-hERG, and a $V_{0.5}$ of 45 ± 4 mV and slope factor of -14 mV (n = 6) for N588K-hERG.

Figure 3: Typical examples of current traces recorded from the drug-block voltage protocol illustrated at top. **A.** WT-hERG, **B.** N588E-hERG, and **C.** N588K-hERG, in the presence of 30 nM cisapride. Dashed lines represent zero current in each case. Note the different scales on each recording; A. and B. are currents recorded during the revelatory voltage step, while C. displays the non-rectifying current of the 3s depolarizing step in N588K-hERG. The percentage of drug-block for each recording was determined by dividing the current measured at the end of the 3s depolarizing step to +20 mV after application of the drug (I_{drug}) by the current measured at the beginning of the recording ($I_{control}$). In the case of WT-hERG and N588E-hERG, the current at this point was determined by fitting an exponential curve to the

first part of the deactivating current during the revelatory voltage step and extrapolating this back to the end of the depolarizing step, as illustrated in A. and B.

Figure 4: Hill Plots of high-affinity hERG blockers. Drug-binding to WT-hERG (■), N588E-hERG (○), and N588K-hERG (●) for **A.** astemizole, **B.** cisapride, **C.** dofetilide **D.** terfenadine. Each data point represents $I_{[drug]} / I_{control}$ ± S.E.M for n= 4-9 cells. **E.** Summary data showing the mean IC_{50} ± S.E.M for each drug. Significant differences between WT-hERG and N588K-hERG are denoted by *. All values are printed in Table 1.

Figure 5: Typical examples of current traces recorded from A. WT-hERG, B. N588E-hERG, and C. N588K-hERG in the presence and absence of 3 μM quinidine. The drug-block voltage protocol is shown at top. Dashed lines represent zero current in each case. Note the >50% of block of N588K-hERG by 3 μM quinidine which is similar to the percentage block in WT-hERG and N588E-hERG. Rates of deactivation in N588E-hERG are faster than WT-hERG due to the use of a -120 mV 'revelatory' voltage step, in order to produce adequate opening of channels to measure current. The rate of deactivation appears to slow in A. and B. with application of drug; this is probably due to some drug unblocking during this step, rather than a true effect on the kinetics of deactivation.

Figure 6: Hill plots of low affinity hERG blockers. Drug-binding to WT-hERG (■), N588E-hERG (○), and N588K-hERG (●) for **A.** quinidine **B.** perhexiline **C.** erythromycin **D.** dl-sotalol. Each data point represents $I_{[drug]} / I_{control}$ ± S.E.M for n= 4-6. **E.** Summary data showing the mean IC_{50} ± S.E.M for each drug. Significant differences between WT-hERG and N588K-hERG are denoted by *. All values are printed in Table 1.

Figure 7A: Conductance voltage curves for S631A-hERG(△), and S620T-hERG(□). Data points are mean ± S.E.M and the curve fitted to the data points is a Boltzmann function. The $V_{0.5}$ of steady state inactivation for the S631A-hERG mutant is 43 ± 2 mV with a slope factor of -16.5 mV (n = 6). S620T-hERG does not inactivate in the voltage range shown (Data from Ficker et al., 1998). Dotted, plain, and dashed lines show data for N588E-hERG, WT-hERG, and N588K-hERG, reproduced from Figure 2.

Figure 7B: The affinity of dofetilide for S631A-hERG (△), and S620T-hERG (□). Dotted, plain, and dashed lines show data for N588E-hERG, WT-hERG, and N588K-hERG respectively, reproduced from Figure 4C. Note the similar drug affinity for the N588K and S631A cell constructs, and the marked right shift (reduced affinity) of dofetilide for the S620T construct.

Figure 8. Markov model of drug-binding to hERG. C_x = closed states. O = open state. I = inactivated state. OD = drug bound to open state. ID = drug bound to inactivated state. Greyed out portions of the model were not altered during modeling simulations.

Figure 9: Dofetilide Hill curves with data points for N588K-hERG and the modeling curve superimposed. Thin plain line, dotted line, and dashed line show WT-, N588K-, and S620T-hERG respectively. The modeled line is thick black. Experimental IC_{50} values for dofetilide block of N588K, and the modeled values respectively: 377 ± 57.8 vs 302 nM.

Figure 10: Hill curves for **A.** astemizole **B.** cisapride **C.** terfenadine and **D.** dl-sotalol with data points for N588K-hERG and the modeling curves superimposed. Thin plain line, dotted line, and dashed line show WT-, N588K-, and S620T-hERG respectively. Modeled lines are

Molecular Pharmacology Fast Forward. Published on August 13, 2008 as DOI: 10.1124/mol.108.049056
This article has not been copyedited and formatted. The final version may differ from this version.

thick black. Experimental IC_{50} values for drug block of N588K and the modeled values respectively: astemizole – 14.8 ± 1.1 vs 13.6 nM; cisapride – 55.9 ± 4.2 vs 77.3 nM; terfenadine – 170 ± 32.3 vs 177 nM; dl-sotalol 1392 ± 266.5 vs 1461 μM. Drug IC_{50} values for S620T-hERG are presented in Table 2; Hill plots for S620T-hERG are presented in the data supplement.

Molecular Pharmacology Fast Forward. Published on August 13, 2008 as DOI: 10.1124/mol.108.049056
This article has not been copyedited and formatted. The final version may differ from this version.

Tables

Table 1: IC_{50} values for the 8 drugs against N588-hERG, WT-hERG and N588K-hERG

	N588E	WT-hERG	N588K
Astemizole	4.8 ± 1.2 nM (5); h = 1.2	5.1 ± 1.4 nM (6); h= 1.0	14.8 ± 1.1 nM (5) *†; h= 0.8
Cisapride	13.9 ± 4.9 nM (4); h = 0.8	20.5 ± 2.2 nM (6); h = 1.0	55.9 ± 4.2 nM (6) *†; h = 0.9
Dofetilide	39.4 ± 7.3 nM (5); h = 1.1	51.0 ± 1.3 nM (9); h = 1.3	377.3 ± 57.8 nM (5) *†; h = 1.3
Terfenadine	48.2 ± 10.6 nM (5); h = 1.0	61.4 ± 16.2 nM (9); h = 1.2	170.2 ± 32.3 nM (7) *†; h =0.9
Quinidine	3.71 ± 0.4 μM (4); h = 1.1	3.2 ± 0.3 μM (5); h = 0.8	3.9 ± 0.3 μM (4); h = 0.9
Perhexiline	5.0 ± 1.8 μM (5); h = 0.8	5.9 ± 0.9 μM (7); h = 1.1	4.7 ± 1.7 μM (5); h = 1.2
Erythromycin	98.4 ± 39.7 μM (5); h = 0.8	129.5 ± 59.9 μM (4); h = 0.7	151.1 ± 49.4 μM (4); h = 0.8
dl-Sotalol	585.6 ± 178.6 μM (4); h = 0.8	515.5 ± 35.5 μM (4); h = 0.9	1392.0 ± 266.5 μM (4) *†; h = 0.9

Table 1: Collated IC_{50} values calculated from the Hill plots in Figure 4 and Figure 6. * denotes a significant difference from N588K to N588E; † denotes a significant difference between N588K and WT-hERG. h = Hill coefficient calculated from the curve of best fit to the data (see Figure 4 and 6). All IC_{50} values are mean ± S.E.M (n cells).

Molecular Pharmacology Fast Forward. Published on August 13, 2008 as DOI: 10.1124/mol.108.049056
This article has not been copyedited and formatted. The final version may differ from this version.

Table 2: Drug Affinity for S620T (IC_{50})

Astemizole	19.8 ± 3.7 nM (n = 10)
Cisapride	157.1 ± 20.2 nM (n = 6)
Dofetilide	3494.4 ± 425.0 nM (n = 4)
dl-Sotalol	2218.2 ± 380.2 uM (n = 5)
Terfenadine	271.8 ± 120.3 nM (n = 4)

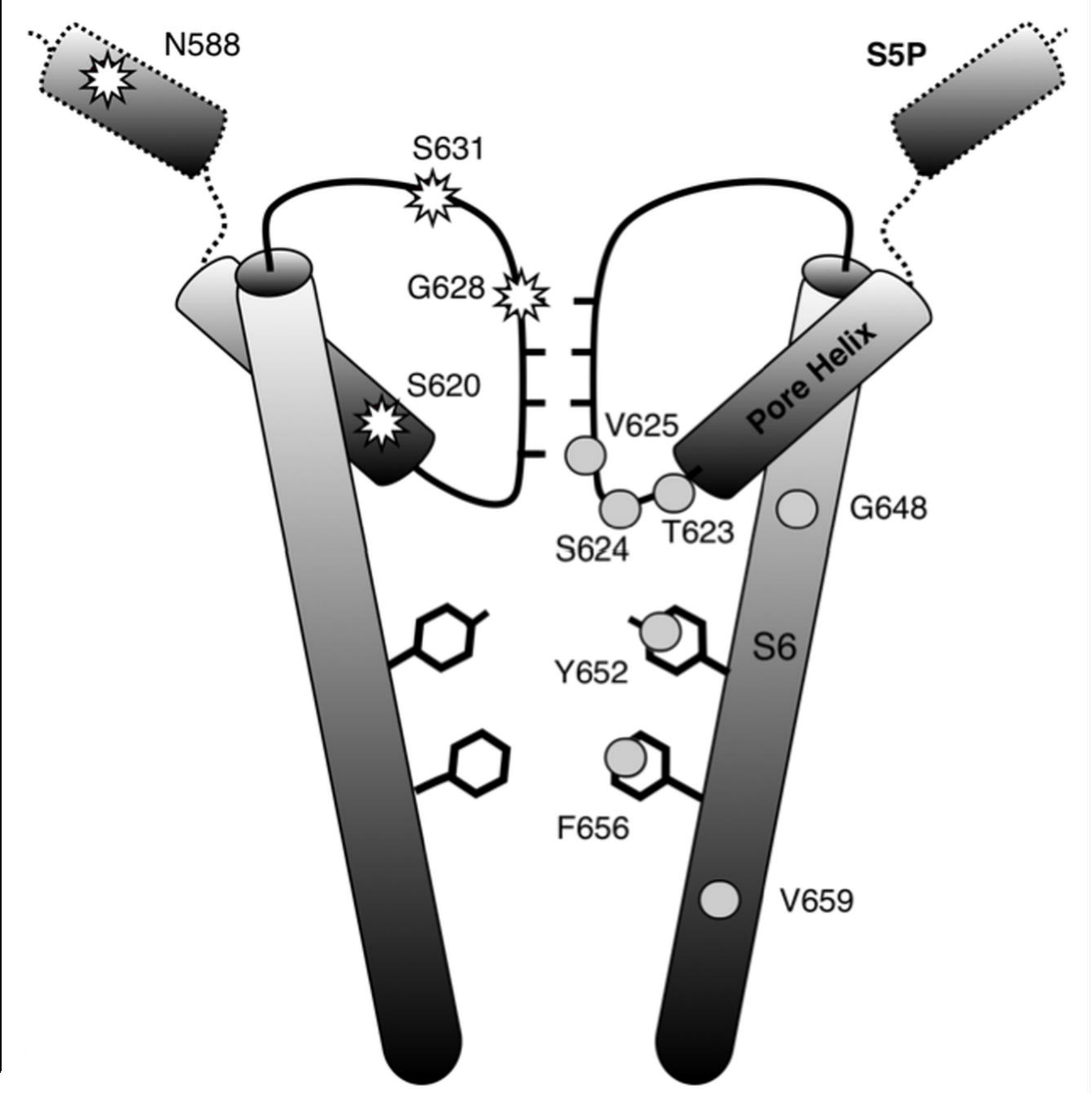
N588
S5P
S631
G628
S620
Pore Helix
V625
G648
T623
S624
S6
Y652
F656
V659

Figure 1.

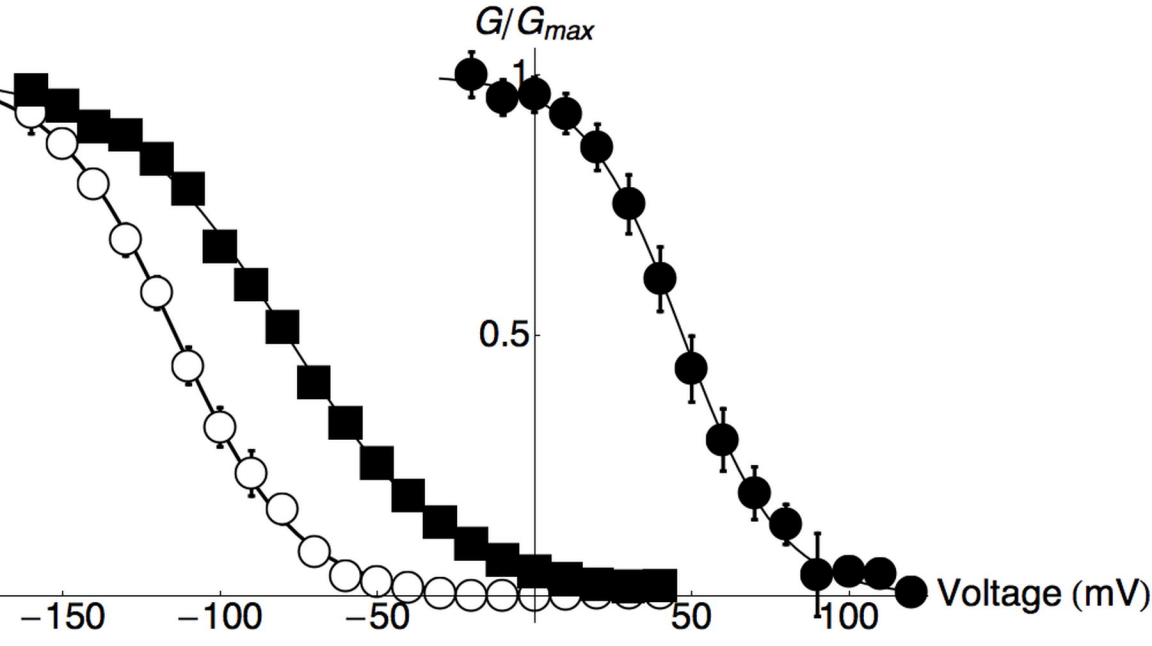

Figure 2.

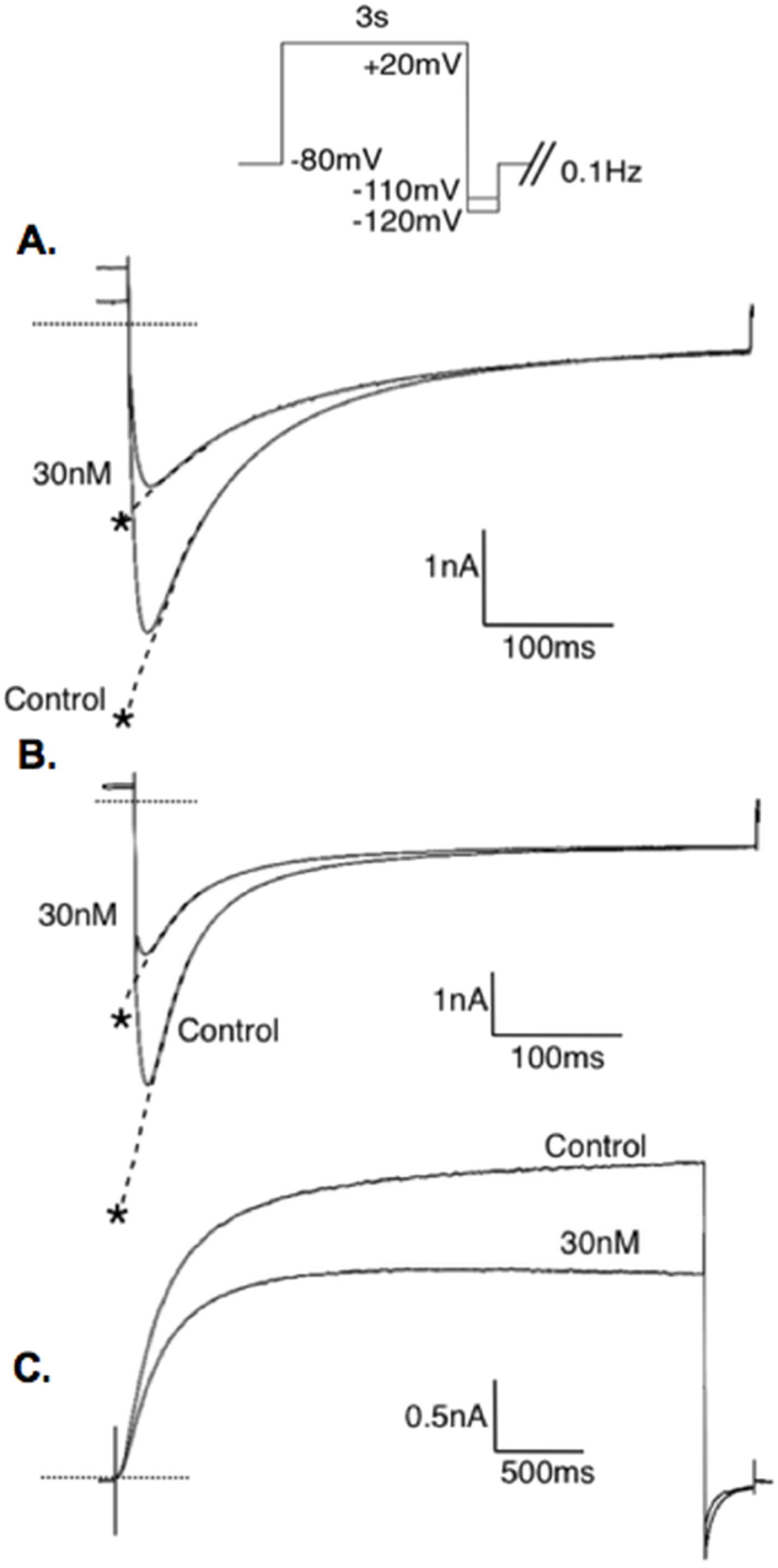
3s
+20mV
-80mV
-110mV
-120mV
0.1Hz
A.
30nM
Control
1nA
100ms
B.
30nM
Control
1nA
100ms
Control
30nM
C.
0.5nA
500ms

Figure 3.

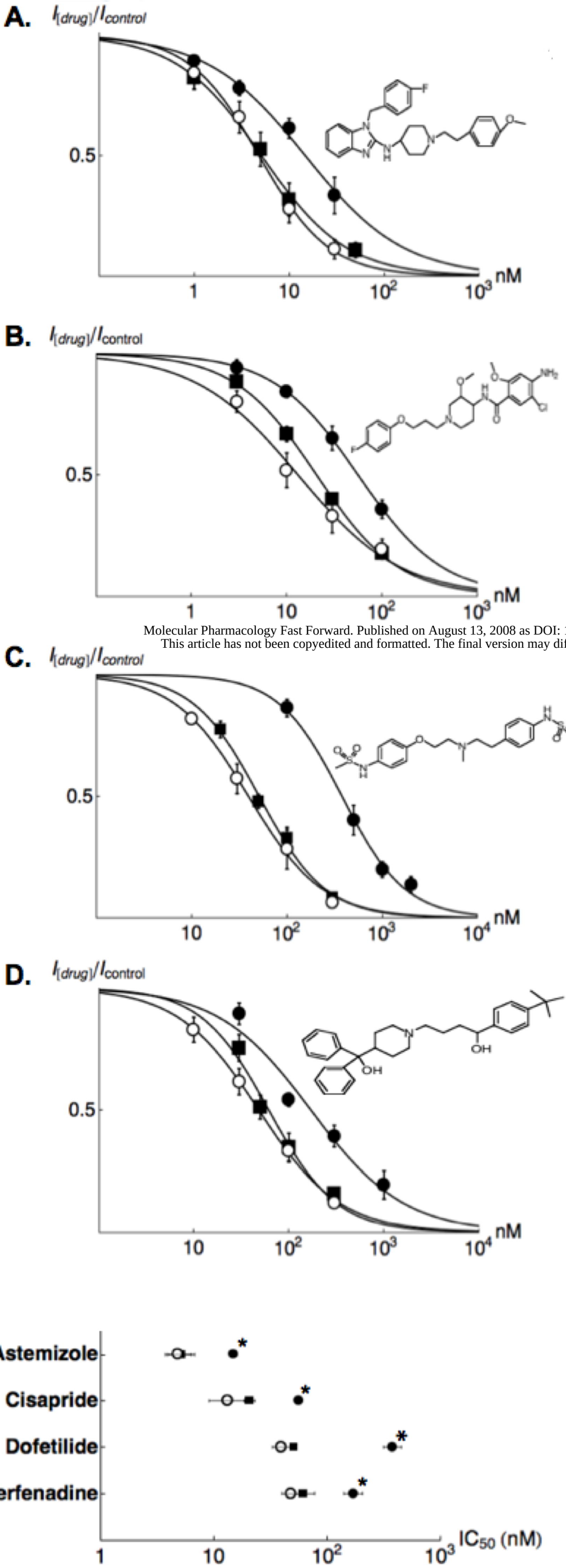

Figure 4.

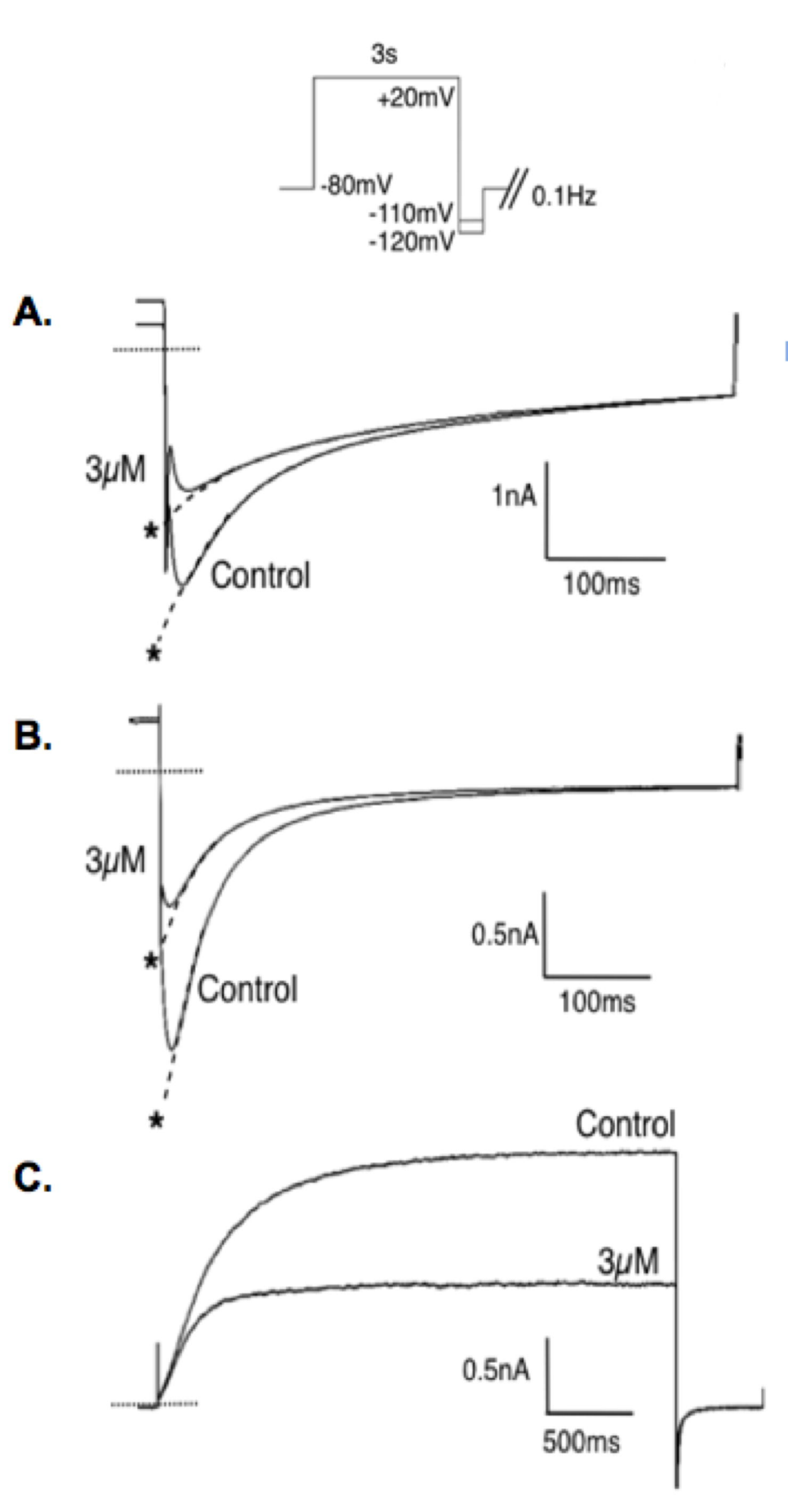
3s
+20mV
-80mV
-110mV
-120mV
0.1Hz
A.
3μM
Control
1nA
100ms
B.
3μM
Control
0.5nA
100ms
C.
Control
3μM
0.5nA
500ms

Figure 5.

Figure 6.

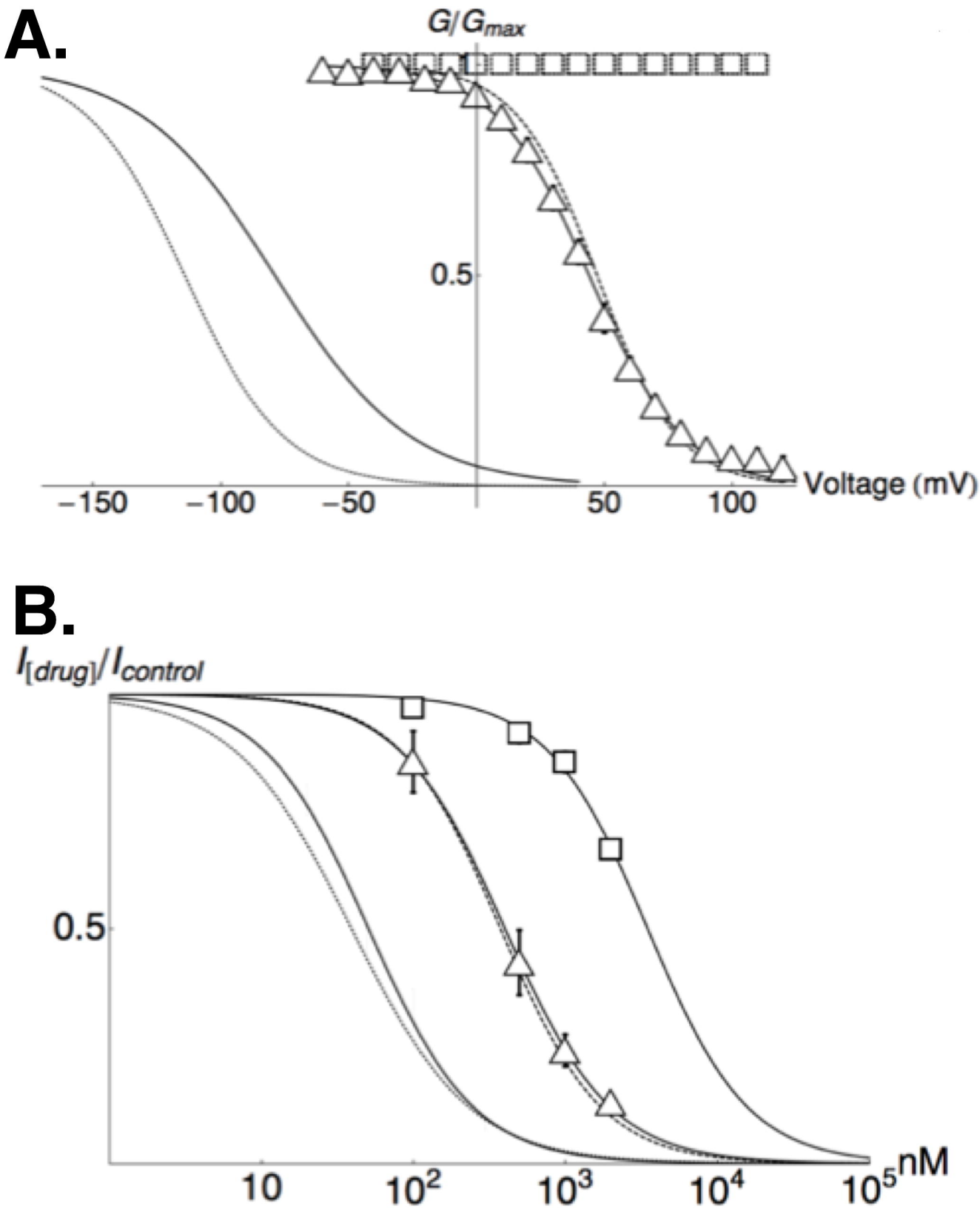
A.
G/G_max
1
0.5
−150
−100
−50
50
100
Voltage (mV)
B.
I_[drug]/I_control
0.5
10
10^2
10^3
10^4
10^5
nM

Figure 7.

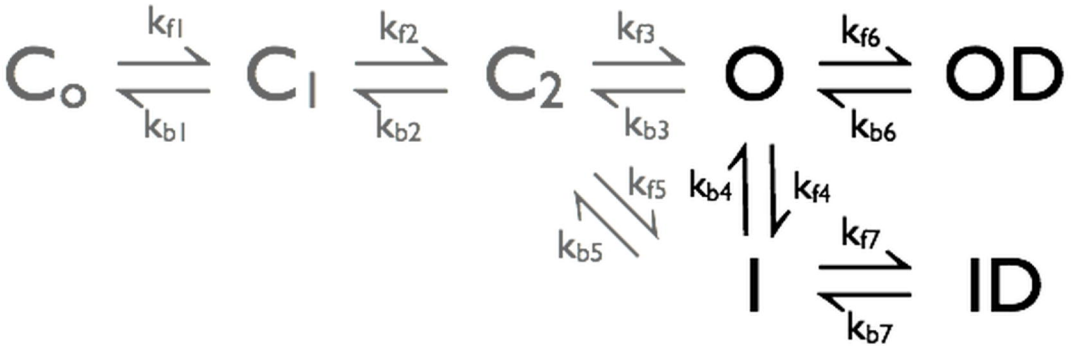
C_o
k_{f1}
k_{b1}
C_1
k_{f2}
k_{b2}
C_2
k_{f3}
k_{b3}
O
k_{f6}
k_{b6}
OD
k_{f5}
k_{b5}
k_{b4}
k_{f4}
I
k_{f7}
k_{b7}
ID

Figure 8

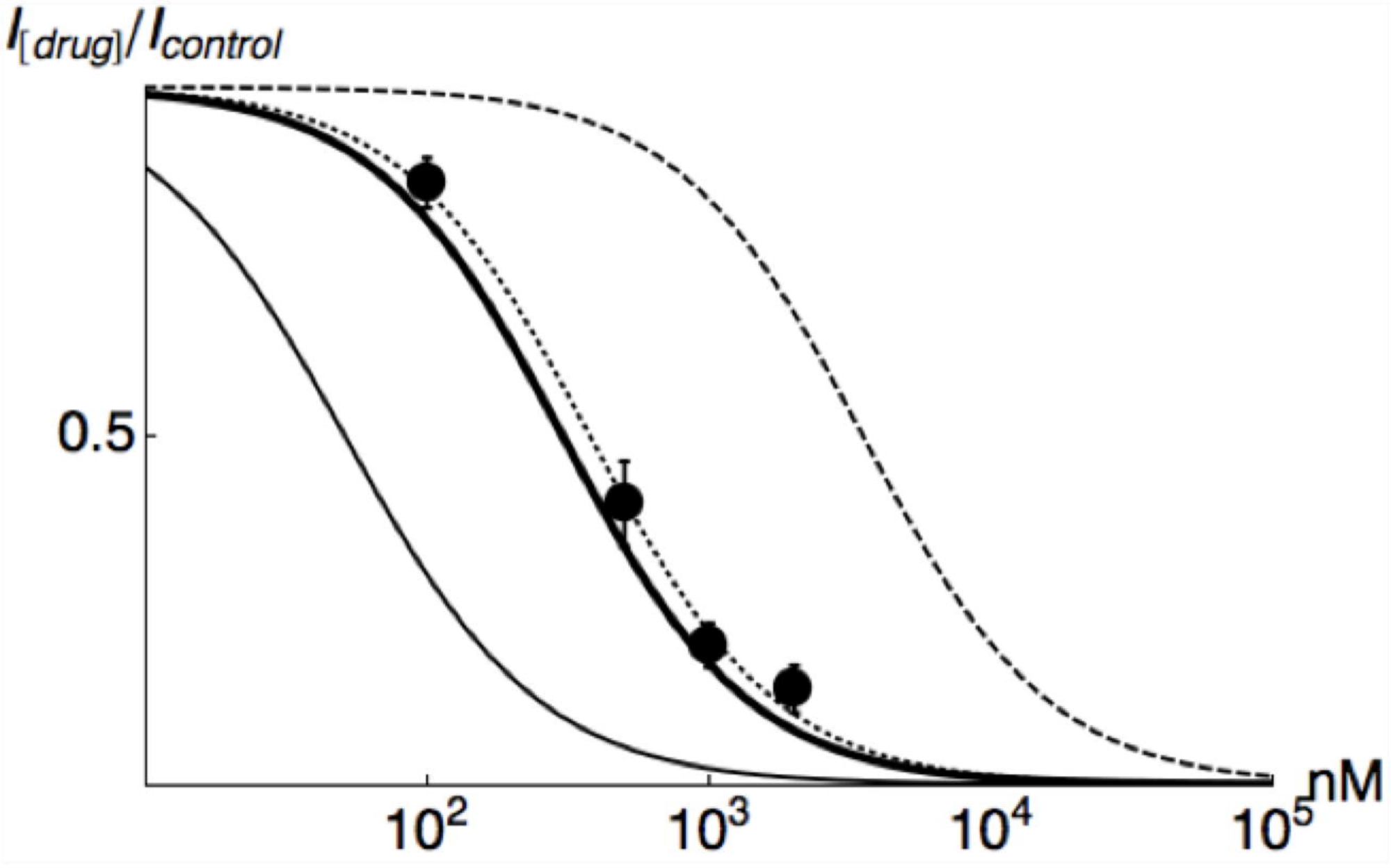

Figure 9.

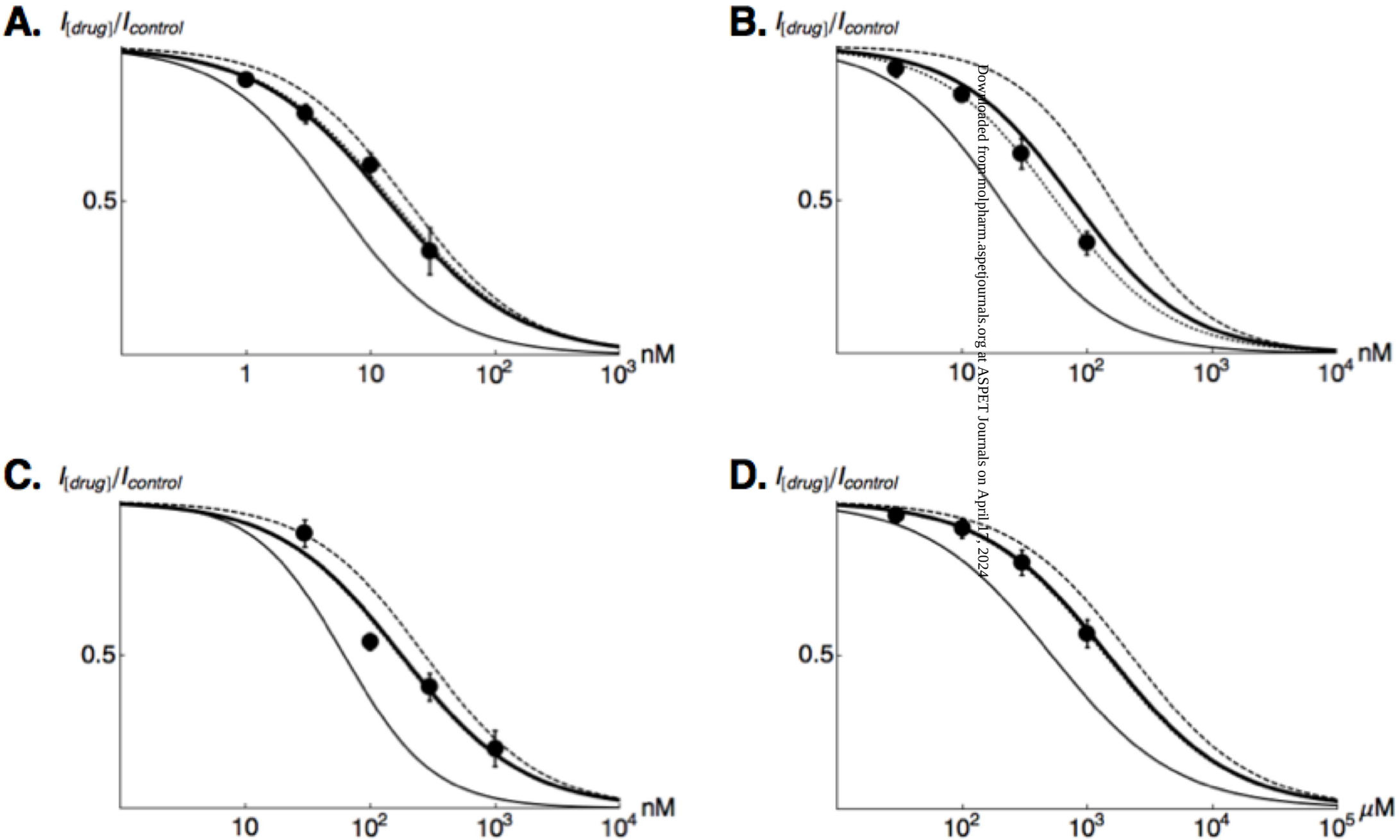

Figure 10.